



## High phosphate content significantly increases apatite formation of fluoride-containing bioactive glasses

Mohammed Mneimne<sup>a</sup>, Robert G. Hill<sup>a</sup>, Andrew J. Bushby<sup>b</sup>, Delia S. Brauer<sup>a,\*</sup>

<sup>a</sup> Unit of Dental Physical Sciences, Barts and The London, Mile End Road, London E1 4NS, UK

<sup>b</sup> Department of Materials, Queen Mary University of London, Mile End Road, London E1 4NS, UK

### ARTICLE INFO

#### Article history:

Received 3 September 2010

Received in revised form 20 October 2010

Accepted 23 November 2010

Available online 27 November 2010

#### Keywords:

Dentifrices

Toothpaste

Fluoride

Bioactive glass

Fluorapatite

### ABSTRACT

Bioactive glass-containing toothpastes for treating dentine hypersensitivity work by precipitating hydroxycarbonate apatite (HCA) onto the tooth surface, but concerns exist over the long-term durability of HCA in the mouth. Fluoride-containing bioactive glasses form fluorapatite (FAP) in physiological solutions, which is more chemically stable against acid attack. The influence of phosphate content on apatite formation was investigated by producing a low-phosphate (about 1 mol% P<sub>2</sub>O<sub>5</sub>) and a high-phosphate (about 6 mol%) series of melt-derived bioactive glasses in the system SiO<sub>2</sub>–P<sub>2</sub>O<sub>5</sub>–CaO–Na<sub>2</sub>O; increasing amounts of CaF<sub>2</sub> were added by keeping the ratio of all other components constant. pH change, ion release and apatite formation during immersion in Tris buffer at 37 °C over up to 7 days were investigated. Crystal phases formed in Tris buffer were characterized using infrared spectroscopy, X-ray diffraction and solid-state nuclear magnetic resonance (NMR) spectroscopy. An increase in phosphate or fluoride content allowed for apatite formation at lower pH; fluoride enhanced apatite formation due to lower solubility of FAp compared to hydroxyapatite or HCA. High phosphate content glasses formed apatite significantly faster (within 6 h) than low phosphate content glasses (within 3 days). In addition, an increase in phosphate content favoured apatite formation rather than fluorite (CaF<sub>2</sub>). <sup>19</sup>F magic angle spinning NMR showed the apatite formed by fluoride-containing glasses to be FAp, which makes these glasses of particular interest for dental applications. This study shows that by varying the phosphate content, the reactivity and apatite formation of bioactive glasses can be controlled successfully.

© 2010 Acta Materialia Inc. Published by Elsevier Ltd. All rights reserved.

### 1. Introduction

Bioactive glasses are known to undergo surface reactions and form a layer of hydroxycarbonate apatite (HCA) on the surface when exposed to body fluids. These glasses have been extensively studied in the literature and have found use as bone substitute materials as they promote bone formation and osseointegration [1]. More recently these glasses have found application in dentistry as a remineralizing additive for toothpastes, particularly for treating dentine hypersensitivity [2,3]. Dentine hypersensitivity is caused by dentinal tubules of root dentine being exposed, and the toothpaste contains bioactive glass with a large fraction of particles small enough (<3 μm) to enter the dentinal tubules. Formation of apatite then occludes the tubules and thus reduces sensitivity. Formation of fluorapatite (FAp) rather than HCA is preferable, as it is more chemically stable at lower pH and would therefore less readily dissolve when the mouth is exposed to acidic conditions (e.g. during consumption of fruit juice and carbonated

beverages). We have recently shown that fluoride-containing bioactive glasses form FAp in simulated body fluid (SBF) [4]. However, the glass component of the toothpaste needs to perform its function and form FAp before it is diluted away by salivary action. Ideally, it should form FAp in the mouth in less than 8 h, corresponding to an overnight period where salivary flow will be minimal. It must also not raise the pH significantly above 7.4 when used at high loadings (up to 10 wt.%) in the toothpaste.

Fluorides have been added to non-fluorine bioactive glass containing toothpastes; however, here the more soluble fluoride salt is likely to give a high fluoride concentration before the calcium concentration is increased by dissolution of the glass and is likely to result in fluorite (CaF<sub>2</sub>) formation, which may inhibit subsequent FAp formation. It is better to deliver Ca<sup>2+</sup>, PO<sub>4</sub><sup>3-</sup> and F<sup>-</sup> ions together in the appropriate amounts to form FAp from a single glass composition in order to avoid the possible formation of CaF<sub>2</sub>.

In bioactive glasses phosphate is present as orthophosphate as shown by <sup>31</sup>P and <sup>29</sup>Si magic angle spinning (MAS) nuclear magnetic resonance (NMR) spectroscopy [5,6]. We hypothesized that an increase in P<sub>2</sub>O<sub>5</sub> content (while adding additional Na<sub>2</sub>O and CaO to maintain a fixed network connectivity (NC) [7]) in fluoride-containing glasses would result in an increase in glass degradation

\* Corresponding author. Tel.: +44 0 207 882 5964; fax: +44 0 207 882 7979.

E-mail address: [d.brauer@qmul.ac.uk](mailto:d.brauer@qmul.ac.uk) (D.S. Brauer).

and ion release and would favour formation of FAp rather than fluorite. We produced two series of glasses in the system  $\text{SiO}_2\text{--P}_2\text{O}_5\text{--CaO--Na}_2\text{O}$ , one with a low phosphate content (about 1 mol%  $\text{P}_2\text{O}_5$ ) and another one with a high phosphate content (about 6 mol%) with increasing concentrations of  $\text{CaF}_2$ . NC was fixed by adding  $\text{CaF}_2$  (rather than substituting for  $\text{CaO}$ ) while the ratio of all other components was kept constant, assuming that fluoride stays associated with calcium, i.e. no Si–F bonds are formed [8,9]. We performed degradation experiments in Tris buffer to demonstrate the effects of glass composition on degradation, pH and in vitro apatite formation of fluoride-containing bioactive glasses.

## 2. Materials and methods

### 2.1. Glass synthesis

Glasses in the system  $\text{SiO}_2\text{--P}_2\text{O}_5\text{--CaO--Na}_2\text{O}$  were prepared using a melt–quench route. A series with low phosphate content (about 1 mol%  $\text{P}_2\text{O}_5$ ) and one with high (about 6 mol%  $\text{P}_2\text{O}_5$ ) were produced.  $\text{CaF}_2$  was added in increasing amounts while NC and the ratio of all other components were kept constant (glasses A–F and A2–F2, Tables 1 and 2). In addition, one sodium-free glass was synthesized for each glass series (glasses H and H2, Tables 1 and 2). Glasses in the high phosphate content series were produced by increasing the phosphate content, whilst adding additional  $\text{Na}_2\text{O}$  and  $\text{CaO}$  in order to maintain a fixed NC.

Mixtures of analytical grade  $\text{SiO}_2$  (Prince Minerals Ltd., Stoke-on-Trent, UK),  $\text{P}_2\text{O}_5$ ,  $\text{CaCO}_3$ ,  $\text{Na}_2\text{CO}_3$  and  $\text{CaF}_2$  (all Sigma–Aldrich, Gillingham, UK) were melted in a platinum–rhodium crucible for 1 h at 1430 °C in an electric furnace (EHF 17/3, Lenton, Hope Valley, UK). A batch size of approximately 100 g was used. After melting, the glasses were rapidly quenched into water to prevent crystallization. After drying, the glass was ground using a vibratory mill (Gyro mill, Glen Creston, London, UK) for 7 min and sieved using a 38  $\mu\text{m}$  mesh analytical sieve (Endecotts Ltd., London, UK). The amorphous structure of the glasses was confirmed by powder X-ray diffraction (XRD; X'Pert PRO MPD, PANalytical, Cambridge, UK; 40 kV/40 mA, Cu  $K_{\alpha}$ , data collected at room temperature).

### 2.2. pH and ion release in Tris buffer

Tris buffer solution was prepared by dissolving 15.090 g tris-(hydroxymethyl)aminomethane (Sigma–Aldrich) in ~800 ml deionized water, adding 44.2 ml 1 M hydrochloric acid (Sigma–Aldrich), heating to 37 °C overnight, adjusting the pH to 7.30 using 1 M hydrochloric acid using a pH meter (Oakton Instruments, Nijkerk, the Netherlands) and filling to a total volume of 2000 ml using deionized water. Tris buffer solution was kept at 37 °C.

50 ml Tris buffer were pipetted into 150 ml polyethylene bottles. pH was measured using a pH meter (Oakton Instruments), and 75 mg of glass powder (<38  $\mu\text{m}$ ) were dispersed in the Tris buffer solution, corresponding to a concentration of 1.5  $\text{g l}^{-1}$ . Experiments were performed in duplicate. Samples were placed in an

**Table 1**  
Nominal glass composition of the low phosphate content glasses in mol%; theoretical network connectivity is 2.13.

Glass	$\text{SiO}_2$	$\text{P}_2\text{O}_5$	$\text{CaO}$	$\text{Na}_2\text{O}$	$\text{CaF}_2$
A	49.47	1.07	23.08	26.38	–
B	47.12	1.02	21.98	25.13	4.75
C	44.88	0.97	20.94	23.93	9.28
D	42.73	0.92	19.94	22.79	13.62
E	40.68	0.88	18.98	21.69	17.76
F	36.83	0.80	17.18	19.64	25.54
H	44.88	0.97	44.87	–	9.28

**Table 2**

Nominal glass composition of the high phosphate content glasses in mol%; theoretical network connectivity is 2.08.

Glass	$\text{SiO}_2$	$\text{P}_2\text{O}_5$	$\text{CaO}$	$\text{Na}_2\text{O}$	$\text{CaF}_2$
A2	38.14	6.33	25.91	29.62	–
B2	36.41	6.04	24.74	28.28	4.53
C2	34.60	5.74	23.51	26.87	9.28
D2	32.95	5.47	22.38	25.59	13.62
E2	31.37	5.21	21.31	24.36	17.76
F2	28.40	4.71	19.29	22.06	25.54
H2	34.60	5.74	50.38	–	9.28

orbital shaker at 37 °C at an agitation rate of 60 rpm for up to 1 week. Tris buffer from the same batch without glass powder was used as control. pH was measured at 1, 3, 7 and 14 days.

After removing the samples from the shaker, pH was measured and solutions were filtered through medium-porosity filter paper (5  $\mu\text{m}$  particle retention, VWR International, Lutterworth, UK) and kept at 4 °C.

Fluoride-release into Tris buffer was measured using a fluoride-selective electrode (Orion 9609BNWP with Orion pH/ISE meter 710, both Thermo Scientific, Waltham, MA, USA). Calibration was performed using standard solutions prepared using Tris buffer to account for ionic strength.

Undiluted solutions (for analysis of phosphorus) as well as samples diluted by a factor 1:5 (for analysis of silicon, sodium and calcium) were acidified using 69% nitric acid and quantitatively analyzed by inductively coupled plasma–optical emission spectroscopy (ICP; Varian Vista-PRO, Varian Ltd., Oxford, UK).

### 2.3. Characterization of glass powders after immersion in Tris buffer

The filter paper was dried at 37 °C and the dried powders were analyzed using Fourier-transform infrared spectroscopy (FTIR; Spectrum GX, Perkin-Elmer, Waltham, MA, USA; data collected from 1600 to 500  $\text{cm}^{-1}$ ) and XRD (data collected at room temperature with a 0.033°  $2\theta$  step size and a count rate of 99.6 s  $\text{step}^{-1}$ , from  $2\theta$  values of 10° to 60°).

$^{19}\text{F}$  MAS NMR experiments on Tris-treated glass powders were performed using a Bruker 200 MHz (4.7 T) spectrometer.  $^{19}\text{F}$  NMR data were collected at a Larmor frequency of 188.2 MHz under spinning conditions of 12.5 kHz in a 4 mm rotor. A low fluorine content probe was used, making background subtraction unnecessary.  $^{19}\text{F}$  chemical shift scale was referenced using the –120 ppm peak of 1 M NaF aqueous solution as a secondary reference against  $\text{CFCl}_3$ .

## 3. Results and discussion

### 3.1. Glass formation

Low phosphate content glasses were obtained in an amorphous state as shown earlier [8]. The XRD patterns of milled high phosphate content glasses A2–F2 (see Supplementary Fig. S1) show amorphous halos, typical of a glassy state. There is evidence of very small amounts of apatite in the sodium-free glass (H2) as shown by the two peaks at 32 and 33° $2\theta$ , and crystallization of small amounts of apatite is likely to have occurred during quenching.

$^{19}\text{F}$  MAS NMR showed previously [8] that by adding  $\text{CaF}_2$  to the composition (and keeping the ratio of all other components constant), rather than substituting it for  $\text{CaO}$ , the NC [10] of the glass and the Q speciation (i.e. the number of bridging and non-bridging oxygens per silicate structural unit) remained unchanged. This contrasts with previous studies on fluoride-containing bioactive glasses [11,12] where  $\text{CaF}_2$  was substituted for  $\text{CaO}$ , which resulted

in a more cross-linked glass and greatly reduced dissolution rate and bioactivity.

### 3.2. Effect of fluoride content on pH of Tris buffer

Soda-lime phosphosilicate-based bioactive glasses (such as Bio-glass® 45S5) are well known to cause a pH rise upon immersion in aqueous solutions [13]. This pH increase favours apatite deposition but can negatively affect the surrounding tissue in vivo, a problem which is largely overlooked in the literature. Too high a pH rise is also a disadvantage for toothpaste applications, as it can negatively affect the oral mucosa.

The fluoride-releasing glasses in this work clearly showed a pH rise within the first 24 h of immersion in Tris buffer (see Fig. 1). The low phosphate content glasses were previously shown to give a similar pH rise in SBF [4]; however, due to the higher buffering capacity of the Tris buffer solution compared to SBF, the pH rise was less pronounced in the current study. Low phosphate glasses showed a further increase in pH (Fig. 1a) between 24 h and 3 days; the pH decrease at day 7 can be explained by a lower initial pH of the Tris buffer solution (7.31 compared to 7.34). By comparison, high phosphate content glasses (Fig. 1b) reached their maximum pH within the first 24 h; after this initial pH rise, the pH stayed constant for the remainder of the experiment.

The pH rise was less pronounced for high phosphate content glasses compared to low phosphate content glasses; the pH values of high phosphate content glasses are between 0.04 and 0.2 lower than the corresponding values for the low phosphate content

glasses. Details are shown for glasses A–F and A2–F2 at 3 days as well as for the two sodium-free compositions (H and H2) over time in Supplementary Fig. S2. The pH values found for sodium-free glasses H and H2 are comparable to those found for glasses C and C2, which are the corresponding sodium-containing glasses. O'Donnell et al. [14] explained the effect of phosphate content on the pH by the release of more phosphate from the glass, which buffers the alkalinity caused by sodium and calcium ions.

The pH rise was also less pronounced with increasing fluoride content in the glass (Fig. 1c and d), both in the low and high phosphate series: There is a small but significant reduction in pH with increasing fluorine content of the glass which mirrors that found for the low phosphate content glasses in SBF [4]. The effect of fluoride content in the glass on the pH in aqueous solution can be explained by ion exchange processes on the glass surface: cations such as  $\text{Na}^+$  or  $\text{Ca}^{2+}$  near the glass surface can go into solution in exchange for  $\text{H}^+$  ions from the solution (from dissociation of water into  $\text{H}^+$  and  $\text{OH}^-$ ), which results in a pH increase. Similarly,  $\text{F}^-$  ions can be exchanged for  $\text{OH}^-$  ions, thereby removing hydroxyl ions from solution; therefore with increasing fluoride content in the glass, the pH rise is less pronounced.

The resulting pH depends on the particle size (i.e. surface area) and the concentration of the glass as well as on the buffering capacity of the surrounding solution, and although the pH values shown here are  $\leq 7.9$  under the experimental conditions in this research, pH values in the oral cavity might potentially be higher depending on the loading of glass in the toothpaste and the amount of saliva present. Our results clearly show the potential

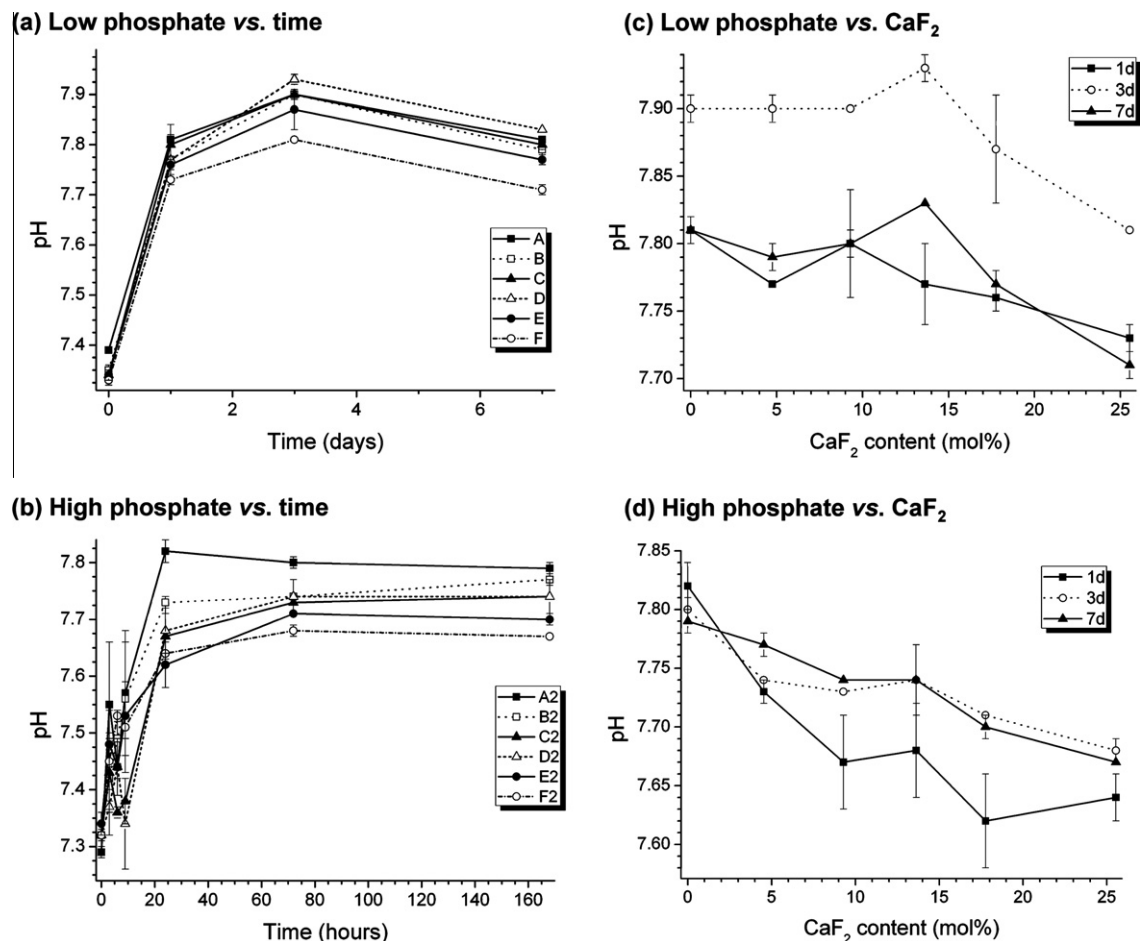


**Fig. 1.** pH of Tris buffer solution after immersion of (a) low phosphate and (b) high phosphate glasses vs. time and (c) low and (d) high phosphate content glass powder vs.  $\text{CaF}_2$  content in the glass. (Lines are drawn as visual guides.)

of increased phosphate and fluoride contents for controlling the pH upon glass degradation.

### 3.3. Apatite deposition in Tris buffer

Conventionally the “bioactivity” (defined as apatite formation) of bioactive glasses is assessed by immersing the glass in SBF, which is a solution saturated in calcium and phosphate, and which mimics the ionic concentrations found in blood plasma [15]. If the glass results in the formation of apatite in the designated time period, it is conventionally termed bioactive. However, the saliva in the mouth is diluted after taking in liquids and is often no longer saturated with regard to  $\text{Ca}^{2+}$  and  $\text{PO}_4^{3-}$ . For this reason we have investigated the apatite-forming ability of the glasses in Tris buffer containing no  $\text{Ca}^{2+}$  and  $\text{PO}_4^{3-}$ , as this represents a more severe test of bioactivity. Formation of apatite was followed using FTIR, XRD and  $^{19}\text{F}$  solid-state MAS NMR.

FTIR spectra of all glass compositions showed significant changes after immersion in Tris buffer in comparison to the spectrum of the unreacted glass (shown in Fig. 2a and b for glasses B and B2, respectively). The bands for the untreated glass powder were mostly due to Si–O vibrational modes: Si–O stretch, Si–O alkali stretch and Si–O bend [16], which will be described in the following. After immersion in Tris buffer, all spectra showed the following changes: disappearance of the non-bridging oxygen (NBO, Si–O<sup>-</sup> alkali<sup>+</sup>) band at  $920\text{ cm}^{-1}$  and sharpening of the Si–O–Si stretch band at about  $103\text{ cm}^{-1}$ . At the same time, new bands appeared at about  $790\text{ cm}^{-1}$ , which were assigned to Si–O–Si bond vibration between two adjacent  $\text{SiO}_4$  tetrahedra as described previously for SBF-treated glasses [4]. These changes

indicate formation of a silica-gel surface layer after leaching of  $\text{Ca}^{2+}$  and  $\text{Na}^+$  ions and formation of Si–OH groups in this ion-depleted glass. Spectra after Tris buffer immersion for 1 week (Fig. 3a and b) showed either a single band or a split band at approximately  $560\text{ cm}^{-1}$ . This is the most characteristic region for apatite and other phosphates, and it corresponds to P–O bonding vibrations in a  $\text{PO}_4^{3-}$  tetrahedron and indicates the presence of crystalline calcium phosphates including hydroxyapatite (HAp) and HCA [16]. A single band in this region suggests the presence of non-apatitic or amorphous calcium phosphate (ACP), which is usually taken as indication of the presence of precursors to apatite [17]. Apatitic  $\text{PO}_4^{3-}$  groups give characteristic split bands at  $560$  and  $600\text{ cm}^{-1}$  [18], with a third signal at  $575\text{ cm}^{-1}$  [19] observed for crystallites of small size. Both glass B and glass B2 (Fig. 2a and b) show the clear presence of a split band in this range at 3 days (glass B) and 6 h (glass B2) which suggests that an increase in phosphate content (from 1.02 mol% in glass B to 6.04 mol% in glass B2) resulted in significantly faster apatite formation. For all glasses showing a split band (Fig. 3a and b), a shoulder is present at  $575\text{ cm}^{-1}$ , indicating the small size of the calcium phosphate crystallites. This is confirmed by crystallite size analysis of apatite formed on bioactive glasses in SBF by O'Donnell et al. [14], which showed crystal sizes in the range of 16 to 26 nm; crystallites in our study are also likely to be in the nanometer size range (below 50 nm).

The presence of carbonate substitution in the apatite is indicated by the band at about  $870\text{ cm}^{-1}$  present in all glasses at 1 week immersion in Tris buffer (Fig. 3a and b). In SBF-treated glass, this carbonate band is usually taken as an indication for carbonate being incorporated into the apatite, resulting in HCA, rather

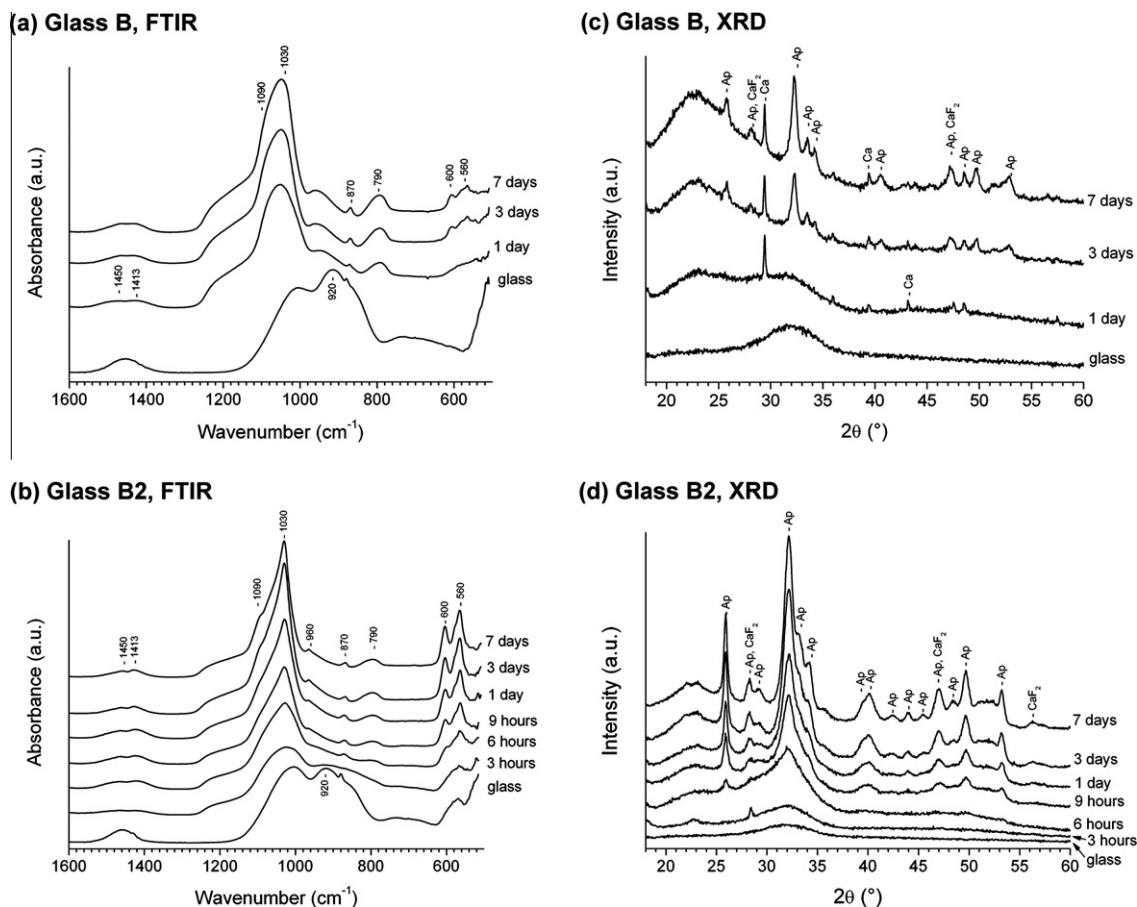
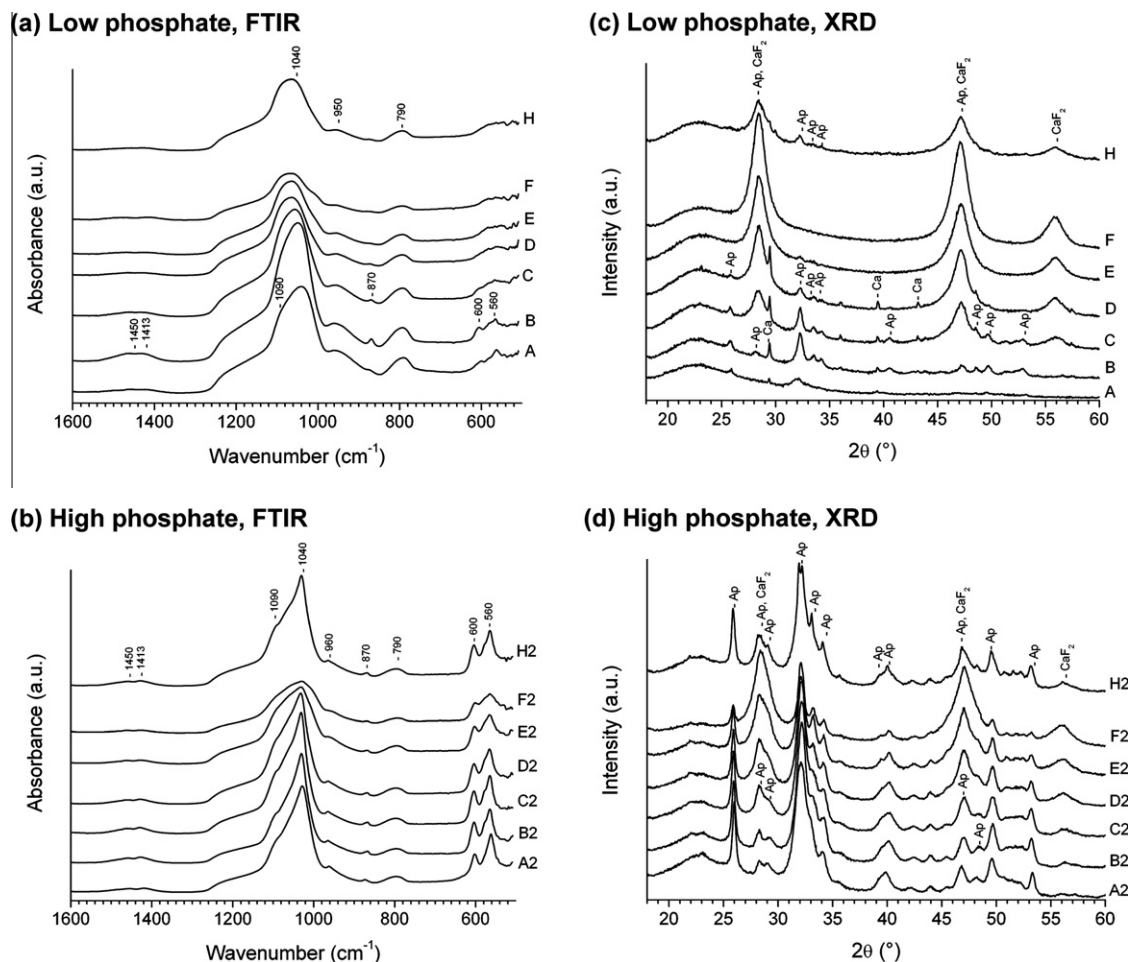


Fig. 2. FTIR spectra (a and b) and XRD patterns (c and d) of glasses B (top, low phosphate) and B2 (bottom, high phosphate) before (“glass”) and after immersion in Tris buffer at different time points.



**Fig. 3.** FTIR spectra (a and b) and XRD patterns (c and d) of low (top) and high (bottom) phosphate content glass powders at 1 week immersion in Tris buffer.

than stoichiometric HAp [20]. It is difficult to distinguish whether this band is split, in which case it would be B-type substitution (i.e. carbonate replacing a phosphate group). However, for most of the compositions treated in Tris buffer for 1 week (Fig. 3a and b) broad  $\text{CO}_3^{2-}$  bands are present in the region starting from  $1410\text{ cm}^{-1}$  which indicates B-type substitution. The  $\text{CO}_3^{2-}$  signal for A-type substitution (i.e. carbonate replacing a hydroxyl group) would be shifted to higher wavenumbers, starting from  $1460\text{ cm}^{-1}$ . Spectra also showed a shoulder at  $1080$  to  $1090\text{ cm}^{-1}$  which corresponds to a P–O stretch which is also observed in B-type substituted HCA [18]. At 1 week, it is most clearly pronounced in the high phosphate content glasses (Fig. 3b), which is consistent with the more clearly pronounced split apatitic bands at  $560$  and  $600\text{ cm}^{-1}$ .

Fig. 2c and d show XRD patterns of glasses B and B2 before (i.e. untreated glass) and at various time points of immersion in Tris buffer. All experimental XRD patterns were compared to reference patterns of hydroxyapatite (JCPDS 09-432), FAp (15-876), HCA (JCPD 19-272) and carbonated FAp (JCPDS 31-267); however, as these patterns overlap we will refer to the pattern of HAp in the following, although phases formed for glasses in the low phosphate content series in SBF were identified to be FAp by  $^{19}\text{F}$  MAS NMR [4].

At 1 day, glass B (Fig. 2c) shows the presence of calcite only (calcium carbonate, JCPD 5-586); at 3 days the typical apatite peaks at  $26^\circ$  and  $32\text{--}34^\circ 2\theta$  appear, superimposed on an amorphous halo. At 1 week, these peaks become larger in intensity and more clearly pronounced. For glass B2 (Fig. 2d) the XRD pattern at 3 h of Tris immersion shows a small peak appearing at

$28.5^\circ 2\theta$ , which might suggest the presence of apatite. However, due to the absence of other characteristic peaks, assigning this peak to a crystal phase is difficult. At 6 h, however, a small peak appears at  $26^\circ 2\theta$  and a broad peak between  $32^\circ$  and  $34^\circ 2\theta$ , all of which are superimposed on an amorphous halo and which clearly indicate presence of apatite. The low peak intensity suggests that the amount of apatite is small, while the line broadening (and the resulting broad feature between  $32^\circ$  and  $34^\circ 2\theta$  rather than clearly resolved individual peaks) is due to the small crystallite size mentioned above. This appearance of apatite Bragg reflections at 6 h is consistent with the presence of characteristic apatitic features in the FTIR spectra of this glass at the same time point (Fig. 2b). At 9 h, additional reflections become visible, and clearly pronounced peaks indicate the presence of apatite; in addition, the position of the amorphous halo has shifted compared to the unreacted glass, due to formation of an ion-depleted glass. This shift in the position of the amorphous halo is also visible for the low phosphate content glass B (Fig. 2c). At later time points, peaks become even more pronounced. Lines are still very broad, indicating the small size and highly disordered character of the crystals.

Fig. 3d shows that at 1 week all high phosphate content glasses (A2–H2) clearly show the presence of apatite by XRD. By contrast, for the low phosphate content glasses (Fig. 3c), peaks of fluorite ( $\text{CaF}_2$ , JCPD 35-816) at  $28^\circ$ ,  $47^\circ$  and  $56^\circ 2\theta$  dominate the XRD pattern for increasing fluoride content. The high phosphate content glasses show the presence of very small amounts of fluorite (Fig. 3d) with increasing fluoride content in the glass. Glass B2 (Fig. 2d) shows a small peak at  $56^\circ 2\theta$ , which could suggest the

presence of small amounts of fluorite in that composition. Fluorite, rather than FAp, forms when the amount of phosphate present relative to those of calcium and fluoride is not sufficient for apatite formation.

Both FTIR and XRD results for the low phosphate content glasses (Figs. 2 and 3c) suggest that the presence of small amounts of fluoride favours apatite formation (as seen by comparing peak intensities for glasses A and B). These results are in contrast to our previous study in SBF, where glass B lacked the typical apatitic features in FTIR and XRD, resulting in our conclusion that the presence of small amounts of fluoride inhibited apatite formation [4]. As FAp shows a much lower solubility compared to HAp or HCA, one would expect small fluoride concentrations to favour apatite deposition, and our results in this study confirm this. The reasons for the previous poorer performance of glass B cannot be fully explained at this stage; however, variation in the amounts or particle sizes of powders used in the XRD study might affect the intensity of the pattern.

Our results show that the formation of apatite occurred more rapidly as the phosphate content increased (Fig. 2c and d), although the NC was kept constant, which indicates that in these glasses the phosphate content is a more important variable than NC (or possibly an overriding factor in a process where NC and phosphate dissolution compete).

Supplementary Fig. S3a shows XRD patterns of glasses C2 and H2 (which is a sodium-free version of glass C2) at 1 week immersion in Tris buffer. While peak intensities are comparable for both compositions, glass H2 shows more clearly pronounced and better resolved peaks: glass C2 shows only a single broad peak at  $32.2^\circ 2\theta$  only; glass H2 shows two peaks at  $31.8^\circ$  and  $32.2^\circ 2\theta$  (JCPDS 09-432) to be clearly resolved (Fig. S3b), indicating a higher degree of crystallinity. In addition, glass H2 clearly shows apatite peaks at 6 h in Tris buffer (Fig. S3c), while glass C2 shows a distorted amorphous halo only at this time point, suggesting the presence of very small amounts of apatite only. This suggests that the all-calcium glass forms apatite significantly faster than the sodium-containing composition, and also forms a more crystalline apatite. One reason for this could be the higher calcium content in glass H2 compared to C2, resulting in an increased release of calcium ions and subsequently increased apatite formation. A similar effect was observed for the low phosphate content glasses in SBF [4]. While the sodium-containing glass C2 would be expected to have a higher solubility (due to  $\text{Na}^+$  ions providing a less efficient cross-linking of the silicate chains compared to  $\text{Ca}^{2+}$  ions, as described previously [4,5]), our results might suggest that the increase in calcium content increases apatite formation despite reduced solubility. However, according to Fig. 3a and c, when tested in Tris buffer, sodium-free low phosphate content glass H does not show increased apatite formation compared to glass C. An alternative explanation for the increased apatite formation of glass H2 compared to C2 is the presence of small amounts of apatite in glass H2 before the glass was treated in Tris buffer (Supplementary Fig. S1). Nucleation is usually the limiting factor in crystallization processes, and these apatite crystals already present in the glass, although low in concentration, can be expected to favour apatite formation compared to a glass which is free of apatite crystals.

A  $^{19}\text{F}$  MAS NMR spectrum (Fig. 4) of glass B2 after 1 week of immersion in Tris buffer shows a clearly pronounced peak at  $-105$  ppm and a shoulder at about  $-90$  ppm. Low phosphate content glasses previously showed the presence of a broad shoulder on the low-frequency side (right-hand side) of the peak between about  $-140$  and  $-150$  ppm, due to a residual glass phase (i.e. due to mixed sodium calcium fluoride species in the glass structure [8]) or due to mixed Ca/Na fluorine complexes adsorbed on the residual glass powder. The absence of a shoulder in this range of

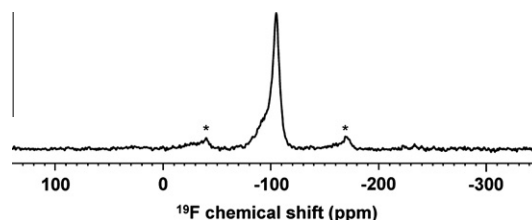


Fig. 4.  $^{19}\text{F}$  MAS NMR spectrum of glass B2 at 1 week immersion in Tris buffer. Spinning side bands are marked by an asterisk.

the spectrum in Fig. 4 suggests that the high phosphate content glass has degraded more compared to the low phosphate content glass, which agrees with our results of increased apatite formation in glass B2 compared to glass B (cf. above). While the cause of the shoulder at  $-90$  ppm cannot be fully explained at this stage and requires detailed further investigation, the signal at  $-105$  ppm was assigned to overlapping peaks of FAp ( $-103$  ppm) and fluorite ( $-108$  ppm), as described previously for low phosphate content glasses treated in SBF [4]. This suggests that the high phosphate content glasses form FAp, rather than HCA or HAp in Tris buffer, similarly to the low phosphate content glasses in SBF. In addition, it shows that despite a significant increase in phosphate content in the glass, we do still see formation of fluorite, which is confirmed by the presence of fluorite peaks in XRD patterns (Figs. 2d and 3d). Fluorite formation can be explained by the fact that experiments were performed in a solution devoid of phosphate ions, in contrast to SBF which contains phosphate concentrations similar to those in physiological solutions. Therefore the phosphate for apatite formation in the present study has to be released from the glass powders. In physiological solutions such as saliva which contain  $\text{PO}_4^{3-}$  (albeit in varying concentrations), the glasses would be expected to perform even better, with formation of fluorite being negligible and apatite formation occurring at even less than 6 h.

It is important to note that structural considerations are a prerequisite when increasing the phosphate content of bioactive glasses for improving degradation and apatite formation. As shown previously, additional network modifier cations (e.g.  $\text{Ca}^{2+}$  or  $\text{Na}^+$ ) need to be added to charge balance the phosphate units ( $\text{PO}_4^{3-}$ ) in the glass [7]. If the phosphate content is increased without additional cations for charge balancing, the silicate network becomes more cross-linked [7], resulting in a reduction in solubility, degradation and apatite formation [14]. Similarly, calcium fluoride needs to be added to the glass composition (thereby keeping the ratio of all other components constant), in order to avoid cross-linking of the silicate network [8] and in order to maintain degradation and bioactivity of the glasses [4,8].

#### 3.4. Glass dissolution and ion release in Tris buffer

For all glasses, elemental concentrations (Fig. 5 for high phosphate content glasses; results for low phosphate glasses follow similar trends and are shown in Supplementary Fig. S4) increase upon glass immersion, which is to be expected as the Tris buffer solution is free of the elements (Ca, P, Na, Si and F) investigated in this study. The use of Tris buffer is often considered of interest for studying the ion-release kinetics of bioactive glasses, as apatite formation (in contrast to studies performed in SBF) is usually not expected. However, as our glasses clearly formed (fluor)apatite in Tris buffer, this has to be taken into account when discussing the ionic concentrations in solution.

Silicon concentrations increase continuously over the time of the experiment, i.e. over 7 days (Figs. 5 and S4). We previously suggested that apatite forms in SBF once Si has reached the solubility

limit, as formation of a silica gel layer is thought to aid nucleation of apatite [4]. However, in this study we see the presence of silica gel as a shifted amorphous halo in XRD within 1 day for glass B and within 6 h for glass B2. Si concentrations, however, keep increasing after these time points, suggesting that the concentration of Si in solution is actually less predictive of silica gel and apatite formation than suggested previously. This confirms results by Lusvardi et al. [12], which also showed that formation of a silica-gel layer is not a prerequisite for apatite formation, and that apatite therefore might precipitate from solution.

Concentrations of Ca, Na and F remain relatively constant after 1 day, while the phosphate concentration drops sharply, confirming our conclusions that the phosphate concentration is critical for apatite formation. Once all the phosphate ions present have been consumed for apatite formation, the concentrations of calcium (between 2 and 3 m mol<sup>-1</sup> and 1.3 and 2 m mol<sup>-1</sup> for the low and high phosphate content glasses, respectively) and fluoride (between 1 and 1.7 m mol<sup>-1</sup> for all glasses) are still high, resulting in formation of fluorite. The fluoride concentrations of the high phosphate content glasses (B2–F2, Fig. 5; results for H2 not shown)

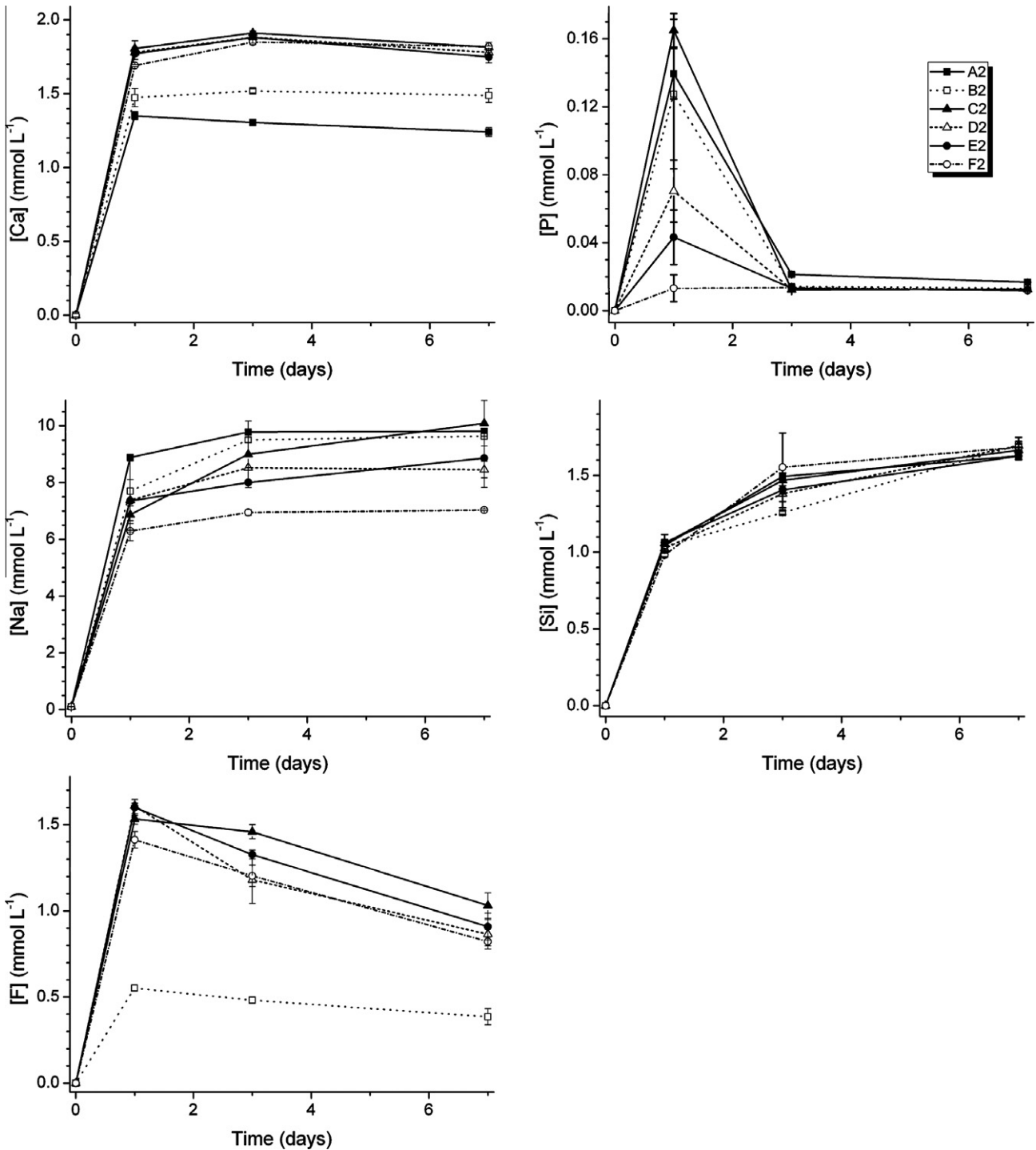
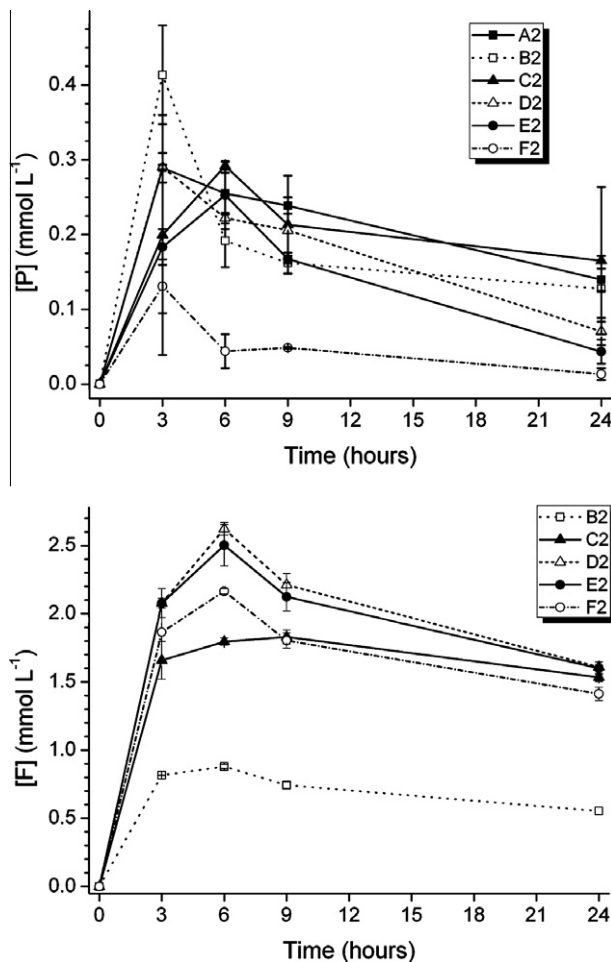


Fig. 5. Elemental concentrations ± standard deviation of Ca, P, Na, Si and F in Tris buffer vs. incubation time of high phosphate content glass powders. (Lines are drawn as visual guides.)



**Fig. 6.** Elemental concentrations  $\pm$  standard deviation of P and F in Tris buffer vs. incubation time up to 24 h of high phosphate content glass powders. (Lines are drawn as visual guides.)

decrease slightly over time. Although the phosphate concentrations at this time point are already low, the further release of small amounts of phosphate from the glass and the immediate formation of FAp with available fluoride ions cannot be excluded.

Fig. 6 shows that for the high phosphate content glasses the calcium and fluoride concentrations reach their maximum within 3 and 6 h, after which the concentrations decrease. This is due to FAp formation at very early time points (i.e. within 6 h).

#### 4. Conclusions

Fluoride-containing bioactive glasses form FAp in Tris buffer solution, which is more acid resistant than HCA. Apatite formation occurred more rapidly (within 6 h) with increased phosphate content in the glass compared to 3 days for low phosphate content glasses. An increase in phosphate content in the glass also favoured formation of FAp rather than fluorite, and allowed for apatite formation at lower pH, which is favourable for applications in both dentistry and orthopaedics. High phosphate content fluoride-containing glasses are particularly suited for use in remineralizing dentifrices for treating dentine hypersensitivity, as the phosphate ions present in saliva should result in apatite formation within even less than 6 h, i.e. well within a typical overnight sleep period of 8 h. Moreover, the design of high phosphate content glasses which are highly bioactive is of great interest also for other appli-

cations such as bone fillers, scaffolds for tissue engineering or coatings of metallic implants. Our results show that the bioactivity of glasses can be increased significantly if glasses are designed based on a good understanding of their structure–property relationship.

#### Acknowledgements

The authors would like to thank Drs. Natalia Karpukhina (Unit of Dental Physical Sciences, Barts and The London, Queen Mary University of London) and Robert V. Law (Department of Chemistry, Imperial College London) for the <sup>19</sup>F MAS NMR spectrum in Fig. 4 and Drs. Kate Peel and Laura Shotbolt (Department of Geography, Queen Mary University of London) for help and support with ICP-OES measurements. Financial support by the Department of Trade and Industry (now the Technology Strategy Board, grant HO669), UK, is gratefully acknowledged.

#### Appendix A. Supplementary data

Supplementary data associated with this article can be found, in the online version, at doi:10.1016/j.actbio.2010.11.037.

#### References

- [1] Hench LL, Paschall HA. Direct chemical bond of bioactive glass–ceramic materials to bone and muscle. *J Biomed Mater Res* 1973;7:25–42.
- [2] Tai BJ, Bian Z, Jiang H, Greenspan DC, Zhong J, Clark AE, et al. Anti-gingivitis effect of a dentifrice containing bioactive glass (NovaMin®) particulate. *J Clin Periodontol* 2006;33:86–91.
- [3] Du MQ, Bian Z, Jiang H, Greenspan DC, Burwell AK, Zhong JP, et al. Clinical evaluation of a dentifrice containing calcium sodium phosphosilicate (NovaMin) for the treatment of dentin hypersensitivity. *Am J Dent* 2008;21:210–4.
- [4] Brauer DS, Karpukhina N, O'Donnell MD, Law RV, Hill RG. Fluoride-containing bioactive glasses: effect of glass design and structure on degradation, pH and apatite formation in simulated body fluid. *Acta Biomater* 2010;6:3275–82.
- [5] Elgayar I, Aliev AE, Boccaccini AR, Hill RG. Structural analysis of bioactive glasses. *J Non-Cryst Solids* 2005;351:173–83.
- [6] Lockyer MWG, Holland D, Dupree R. NMR investigation of the structure of some bioactive and related glasses. *J Non-Cryst Solids* 1995;188:207–19.
- [7] O'Donnell MD, Watts SJ, Law RV, Hill RG. Effect of P<sub>2</sub>O<sub>5</sub> content in two series of soda lime phosphosilicate glasses on structure and properties – part I: NMR. *J Non-Cryst Solids* 2008;354:3554–60.
- [8] Brauer DS, Karpukhina N, Law RV, Hill RG. Structure of fluoride-containing bioactive glasses. *J Mater Chem* 2009;19:5629–36.
- [9] Lusvardi G, Malavasi G, Cortada M, Menabue L, Menziani MC, Pedone A, et al. Elucidation of the structural role of fluorine in potentially bioactive glasses by experimental and computational investigation. *J Phys Chem B* 2008;112:12730–9.
- [10] Hill R. An alternative view of the degradation of bioglass. *J Mater Sci Lett* 1996;15:1122–5.
- [11] Hench LL, Spilman DB, Hench JW, inventors. University of Florida, assignee. Fluoride-modified bioactive glass (Bioglass) and its use as implant material. US patent 4775646. 1988 Oct 4.
- [12] Lusvardi G, Malavasi G, Menabue L, Aina V, Morterra C. Fluoride-containing bioactive glasses: surface reactivity in simulated body fluids solutions. *Acta Biomater* 2009;5:3548–62.
- [13] Aina V, Malavasi G, Pla AF, Munaron L, Morterra C. Zinc-containing bioactive glasses: surface reactivity and behaviour towards endothelial cells. *Acta Biomater* 2009;5:1211–22.
- [14] O'Donnell MD, Watts SJ, Hill RG, Law RV. The effect of phosphate content on the bioactivity of soda-lime-phosphosilicate glasses. *J Mater Sci Mater Med* 2009;20:1611–8.
- [15] Kokubo T, Kushitani H, Sakka S, Kitsugi T, Yamamuro T. Solutions able to reproduce in vivo surface-structure changes in bioactive glass–ceramic A-W. *J Biomed Mater Res* 1990;24:721–34.
- [16] Kim CY, Clark AE, Hench LL. Early stages of calcium–phosphate layer formation in bioglasses. *J Non-Cryst Solids* 1989;113:195–202.
- [17] Jones JR, Sepulveda P, Hench LL. Dose-dependent behavior of bioactive glass dissolution. *J Biomed Mater Res* 2001;58:720–6.
- [18] LeGeros RZ, Trautz OR, Klein E, LeGeros JP. 2 Types of carbonate substitution in apatite structure. *Experientia* 1969;25:5–7.
- [19] Rey C, Combes C, Drouet C, Lebugle A, Sfihi H, Barroug A. Nanocrystalline apatites in biological systems: characterisation, structure and properties. *Materialwiss Werkst* 2007;38:996–1002.
- [20] Lu X, Leng Y. Theoretical analysis of calcium phosphate precipitation in simulated body fluid. *Biomaterials* 2005;26:1097–108.